Theor Chem Acc (2000) 104:240–246
DOI 10.1007/s002140000131

Theoretical
Chemistry Accounts

*Regular article*

# A density functional theory study of the chemoselectivity and regioselectivity of the domino cycloaddition reactions of nitroalkenes with substituted alkenes

**Luis R. Domingo**

Departamento de Química Orgánica, Universidad de Valencia, Dr. Moliner 50, 46100 Burjassot, Valencia, Spain

Received: 16 September 1999 / Accepted: 3 February 2000 / Published online: 2 May 2000


**Abstract.** The chemoselectivity and regioselectivity of the domino intermolecular [4 + 2]/[3 + 2] cycloaddition reactions of nitroalkenes with substituted alkenes, vinyl ethers as electron-rich alkenes and vinyl ketones as electron-poor alkenes, have been studied using density functional theory (DFT) methods with the B3LYP functional and the 6-31G* basis set. These domino processes comprise two consecutive cycloaddition reactions: the first one is an intermolecular [4 + 2] cycloaddition of the vinyl ether to the nitroalkene to give a nitronate intermediate, which then affords the final nitroso acetal adduct through an intermolecular [3 + 2] cycloaddition reaction with the vinyl ketone. The two consecutive cycloadditions present total chemoselectivity and ortho regioselectivity. While first [4 + 2] cycloaddition reaction takes place along the attack of the electron-rich alkene to nitroalkene, the [3 + 2] one takes place along the attack of the electron-poor alkene to the corresponding nitronate intermediate. This DFT study is in complete agreement with the experimental results.

**Key words:** Domino cycloadditions – Chemoselectivity – Regioselectivity – Molecular mechanisms – DFT

## 1 Introduction

Domino cycloadditions play a key role in organic syntheses where construction of complex polycyclic structures with adequate regio- and stereochemical control is needed [1–4]. In this type of process, several bonds of the target molecule are formed alongside a continuous sequence of reactions which does not require isolation of intermediates, changes in reaction conditions or addition of reagents. The interest in this subject is shown by numerous recent reviews [3, 5, 6].

Among domino-type reactions, those involving nitroalkenes have been extensively developed for the stereoselective construction of polycyclic nitrogen-containing compounds [5]. Denmark and Thorarensen [5] have concentrated on Lewis acid catalyzed intermolecular [4 + 2]/intramolecular [3 + 2] cycloadditions of nitroalkenes with chiral vinyl ethers for the construction of polycyclic nitrogen bases. These domino reactions take place with total regioselectivity and with high stereoselectivity to obtain mainly a final cycloadduct along with the formation of six stereogenic centers, three of which are controlled by the outcome of the first cycloaddition.

Recently, Avalos et al. [7] have studied the domino intermolecular [4 + 2]/[3 + 2] cycloaddition reaction of a carbohydrate-based nitroalkene **I** with ethyl vinyl ether **II** in ethanolic solution without a catalyst, which yields a single diastereomer **III** (Scheme 1). This domino cyclo-

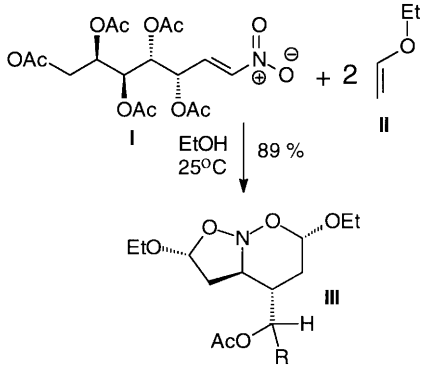


**Scheme 1**

addition takes place with total ortho regioselectivity; the [4 + 2] cycloaddition is endo selective, while the [3 + 2] one is exo selective.

More recently, Avalos and coworkers [8, 9] have reported the domino intermolecular [4 + 2]/[3 + 2] cycloaddition reaction of nitroalkene **I** with ethyl vinyl ether as an electron-rich alkene and methyl vinyl ketone (MVK) **IV** as an electron-poor alkene (Scheme 2). This three-component domino reaction takes place with total chemo-, regio-, facial- and stereoselectivity to obtain

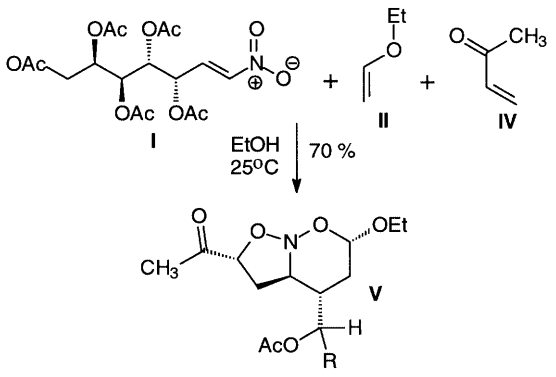


Scheme 2

mainly a single diastereomer **V** along with the formation of five stereogenic centers. As for the aforementioned domino reaction, this process takes place along an endo/ortho attack of ethyl vinyl ether to the nitroalkene, followed of an exo/ortho attack of MVK to the corresponding nitronate intermediate to give the final nitroso acetal cycloadduct.

Despite the obvious potential of these domino processes and their many variations, the reaction pathways have not been studied theoretically so far. A deep knowledge of the molecular mechanism is fundamental, however, for a rationalization of the experimental results. Recently, we described a PM3 semiempirical study for the domino reaction of nitroalkene **VI** with the silyl vinyl ether **VII** to give the nitroso acetal cycloadduct **VIII** (Scheme 3) [10]. For this domino reaction the presence of both silyl and methyl ether in the electron-rich alkene increases the nucleophilic character of the silyl vinyl ether, allowing a stepwise mechanism for the first cycloaddition, which is enhanced with the inclusion of a Lewis acid catalyst and solvent effects [10]. The use of a nonchiral methyl vinyl ether (MVE) together with a small Lewis acid catalyst, $Al(CH_3)_3$, affords a large endo selectivity [10].

In the present work a density functional theory (DFT) study of the chemoselectivity and regioselectivity of the domino intermolecular [4 + 2]/[3 + 2] reaction of nitroethene, **R1**, with MVE, **R2**, and MVK, **R3**, to yield the nitroso acetal adduct **P3** is carried out, as a model of the three-component domino reaction reported by Avalos and coworkers [8, 9] (Scheme 4). Our purpose is to contribute to a better mechanistic understanding of this sort of intermolecular domino process, especially by characterization of the stationary points on the reactive potential-energy surface (PES).

## 2 Computing methods

In recent years, theoretical methods based on DFT [11, 12] have emerged as an alternative to traditional ab initio methods in the study of the structure and reactivity of chemical systems. Diels–Alder reactions and related reactions have been the object of several density functional studies showing that functionals that include

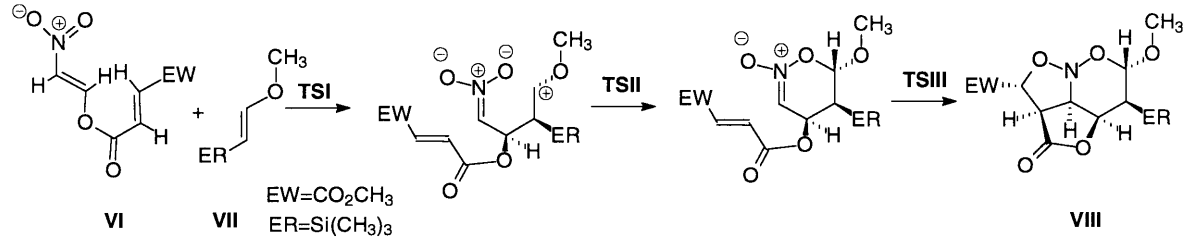


Scheme 3

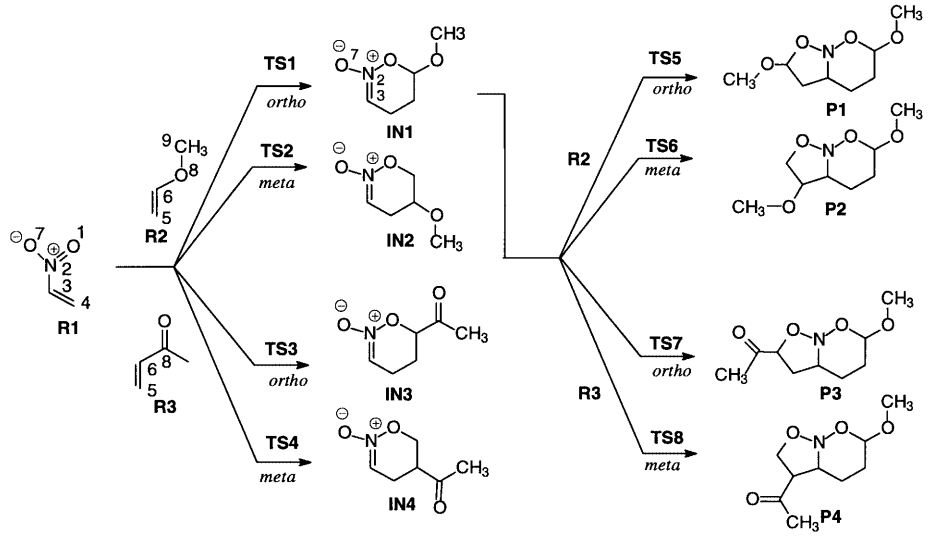


Scheme 4

gradient corrections and hybrid functionals, such as the gradient corrected functional of Becke and Lee, Yang and Parr (B3LYP), together with the 6-31G* basis set, lead to potential-energy barriers (PEBs) in good agreement with the experimental results [13–26]. In the present study geometrical optimizations of the stationary points along the PES were carried out using B3LYP [27, 28] for exchange and correlation, with the standard 6-31G* basis set [29]. The stationary points were characterized by frequency calculations in order to verify that minima and transition structures have zero and one imaginary frequency, respectively. The optimizations were carried out using the Berny analytical gradient optimization method [30, 31]. We used the simplified model **R1** instead of the chiral carbohydrate-based nitroalkene **I** used by Avalos and coworkers [8, 9]. Several conformational structures related to the rotation of the methyl group of the methyl ether and methyl ketone at the transition structures (TSs) were considered and the most stable ones were chosen. Optimized geometries of all the structures are available from the author. The electronic structures of the stationary points were analyzed by the natural bond orbital (NBO) method [32, 33]. All calculations were carried out with the Gaussian 98 suite of programs [34].

## 3 Results and discussion

### *3.1 Energies*

The domino reaction between nitroethene, **R1**, and the substituted alkenes **R2** and **R3** can take place along several competitive reaction channels which involve two consecutive intermolecular cycloaddition reactions (Scheme 4). The first process is a [4 + 2] cycloaddition between **R1** and **R2** or **R3** to give a nitronate intermediate, while the second one is a [3 + 2] cycloaddition of this intermediate with **R2** or **R3** to give the final nitroso acetal adduct.

The [4 + 2] cycloaddition between **R1** and **R2** or **R3** can take place along four reactive channels with each one corresponding to the endo/exo approaches of the substituted alkenes in two regioisomeric possibilities, the ortho (head-to-head) and meta (head-to-tail) ones. Since in the present study the stereoselectivity was been considered, we chose the most favorable endo/exo approach for each regioisomeric possibility.[1] As a consequence, four TSs were considered, **TS1**, **TS2**, **TS3** and **TS4**, corresponding to the ortho and meta approach modes of **R2** and **R3** to **R1**, respectively.

For the second [3 + 2] cycloadditions eight attack modes of the two dipolarophiles, **R2** and **R3**, are possible for each intermediate. These attack modes are related to the endo and exo approaches of the substituted alkenes in the two regioisomeric possibilities, ortho and meta, and for each of the two faces of the quiral nitronates obtained along the first [4 + 2] cycloadditions. As for the first [4 + 2] cycloadditions, we studied only the regioselectivity of the cycloadditions of the two dipolarophiles to the most favorable nitronate intermediate **IN1** obtained form the first stage. As a consequence, four TSs were considered for the second cycloadditions, **TS5**, **TS6**, **TS7** and **TS9**, corresponding to the ortho and meta approach modes of **R2** and **R3** to **IN1**, respectively.

A schematic representation of the stationary points along the reactive channels is presented in Scheme 4, together with the atom numbering. The total and relative electronic energies are given in Table 1, while Figs. 1 and 2 present the geometries of the TSs corresponding to the intermolecular [4 + 2] and [3 + 2] cycloadditions, respectively. A schematic representation of the different energy profiles is depicted in Fig. 3.

The PEBs associated with the [4 + 2] cycloadditions of nitroethene, **R1**, with MVE, **R2**, are 12.0 kcal/mol (**TS1**) and 30.2 kcal/mol (**TS2**), while the PEBs associated with the cycloadditions with MVK, **R3**, are 21.5 kcal/mol (**TS3**) and 26.1 kcal/mol (**TS4**). These data indicate that for the first cycloaddition the most favorable reaction channel corresponds to the ortho addition of the electron-rich MVE to nitroethene. The energetic difference between the most favorable reaction channels for the addition of **R2** and **R3** to **R1** is 9.5 kcal/mol, indicating that this cycloaddition is very chemoselective. Moreover, the energetic difference between the ortho and meta reaction channels for the cycloaddition between **R1** and **R2**, **TS1** and **TS2**, is 18.2 kcal/mol. As a consequence, this cycloaddition also has total ortho regioselectivity. The unexpected cycloaddition between **R1** and **R3** also has ortho regioselectivity, **TS3** being 4.6 kcal/mol more favorable than **TS4**.

These [4 + 2] cycloadditions, which conduce to the formation of the nitronate intermediates **IN1**, **IN2**, **IN3** and **IN4** are very exothermic processes, in the range from −11 to −22 kcal/mol. The larger stability of the intermediate **IN1** is due to an anomeric effect that appears between the O1 oxygen atom of the nitronate group and the axial O8 oxygen atom of the methyl ether [35].

The nitronate intermediate **IN1** carries out the next intermolecular [3 + 2] cycloadditions with **R2** and **R3**, which act as dipolarophiles, to give the final cycloadducts **P1**, **P2**, **P3** and **P4**. The PEBs associated with the [3 + 2] cycloadditions of **IN1** with MVE are 12.3 kcal/mol (**TS5**) and 19.7 kcal/mol (**TS6**), while the PEBs associated with the cycloadditions with MVK are 9.4 kcal/mol (**TS7**) and 12.8 kcal/mol (**TS8**). These data indicate that the more favorable reaction channel corresponds to the ortho addition of the electron-poor MVK to the nitronate **IN1**. The energetic difference between the most favorable reaction channel for the addition of **R2** and **R3** to **IN1** is 2.9 kcal/mol, indicating that the second cycloaddition of this domino reaction is also chemoselective. This low energy difference justifies that the domino reaction can also take place in the absence of MVK (Scheme 1) [7]. The energetic difference between the ortho and meta reaction channels for the [3 + 2] cycloadditions between **IN1** and **R3**, **TS7** and **TS8**, is 3.4 kcal/mol; as a consequence, this cycloaddition reaction also has ortho regioselectivity, in agreement with the experimental results [8, 9].

The [4 + 2] cycloaddition is more regioselective than the [3 + 2] one. (The energy difference between **TS1** and **TS2** is 18.2 kcal/mol, while for **TS7** and **TS8** it is 3.4 kcal/mol). This fact is in agreement with the poor regioselectivity found for the 1,3-dipolar cycloadditions

[1] The endo/exo sterereoselectivity for these cycloaddition processes has been studied previously using PM3 semiempirical methods. While the additions of **R2** to **R1** shows an endo selectivity [26], the other reactive channels are exo selectives. These results are in agreement with the experimental results [8, 9]

**Table 1.** B3LYP/6-31G* total energies including the zero-point energy (au) and relative energies for the [4 + 2] cycloadditions relative to **R1** and **R2** or **R3** and for the [3 + 2] cycloadditions relative to **IN1** and **R2** or **R3** (kcal/mol, in *parentheses*) for the stationary points of the domino cycloaddition reaction between the nitroalkene **R1** and the enol ether **R2** and the vinyl ketone **R3**

| | | | | | |
|---|---|---|---|---|---|
| **R1** | −283.033797 | | | | |
| **R2** | −193.027379 | | | | |
| **R3** | −231.147164 | | | | |
| **TS1** | −476.041992 | (12.0) | **TS5** | −669.104245 | (12.3) |
| **TS2** | −476.013115 | (30.2) | **TS6** | −669.092435 | (19.7) |
| **TS3** | −514.146704 | (21.5) | **TS7** | −707.228603 | (9.4) |
| **TS4** | −514.139409 | (26.1) | **TS8** | −707.223127 | (12.8) |
| **IN1** | −476.096432 | (−22.1) | **P1** | −669.168328 | (−27.9) |
| **IN2** | −476.081474 | (−12.7) | **P2** | −669.154480 | (−19.2) |
| **IN3** | −514.206368 | (−15.9) | **P3** | −707.277910 | (−21.5) |
| **IN4** | −514.199475 | (−11.6) | **P4** | −707.272712 | (−18.3) |

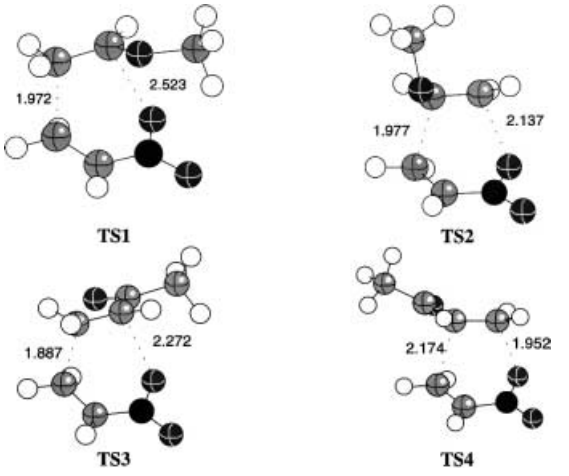


**Fig. 1.** Transition structures corresponding to the [4 + 2] cycloadditions between the nitroalkene **R1** and the substituted alkenes **R2** and **R3**. The values of the bond lengths directly involved in the processes are given in angstroms

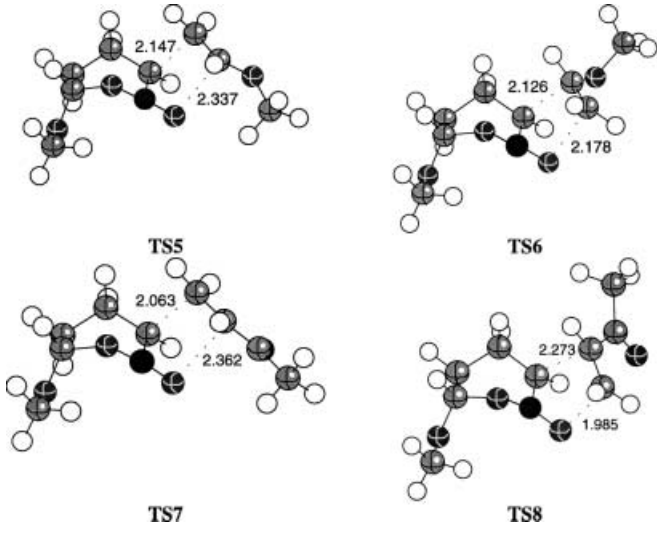


**Fig. 2.** Transition structures corresponding to the [3 + 2] cycloadditions between the intermediate **IN1** and the substituted alkenes **R2** and **R3**. The values of the bond lengths directly involved in the processes are given in angstroms

compared with the counterpart Diels–Alder ones [36, 37].

These [3 + 2] cycloadditions, which conduce to the formation of four final cycloadducts, **P1**, **P2**, **P3** and **P4**, are very exothermic processes, in the range from −18 to −28 kcal/mol; the global process for the formation of the final cycloadduct **P3** is very exothermic, −43.6 kcal/mol. Moreover, this DFT study gives the intermediate **IN1** as an unstable nitronate intermediate; the PEB for the second stage is lower than that for the first one. As a consequence, as **IN1** is formed along the first [4 + 2] cycloaddition, it reacts quickly with **R3** to give **P3**.

### *3.2 Geometrical parameters and frequency analysis*

For the ortho [4 + 2] cycloaddition processes the lengths of the O1—C6 and C4—C5 forming bonds at the TSs are 2.523 and 1.972 Å at **TS1** and 2.272 and 1.887 Å at **TS3**, respectively, while for the meta ones the lengths of the O1—C5 and C4—C6 forming bonds at the TSs are 2.137 and 1.977 Å at **TS2** and 1.952 and 2.174 Å at **TS4**, respectively. These geometrical parameters indicate that the asynchronicity of these bond formation processes depends on both regioisomeric approaches and on the nature of the dienophile. The ortho approaches are more asynchronous than the meta ones; the reaction with MVE leads to the most asynchronous TS, **TS1**.

It is interesting to note the different arrangement of the methyl ether group in **TS1** and **TS2** (Fig. 1). While for the former this adopts an antiperiplanar arrangement [10, 26], the C9—O8—C6—C5 dihedral angle is 166° at **TS1**, for the later it adopts a nonplanar arrangement, the C9—O8—C6—C5 dihedral angle is −90° at **TS2**. These features are due to two different behaviors of the lone pair of the O8 oxygen atom at the corresponding TSs. For **TS1**, the periplanar arrangement of the methyl ether group increases the nucleophilic character of MVE along the ortho approach by a favorable $\pi$ delocalization of the lone pair, which is located on a $p_z$ atomic orbital of the oxygen atom, on the C5—C6 double bond of MVE [10, 26]. However, along the meta approach MVE behaves as a dienophile rather than a nucleophile, and the electronic repulsion that appears between the lone pair and the C4—C5 forming bond demands a nonperiplanar arrangement of the methyl group in order to minimize the unfavorable electronic repulsion. The $\pi$ delocalization that appears along the ortho approach is in agreement with the shortening of

the C6—O7 bond length at **TS1** (1.319 Å) relative to that at **TS2** (1.392 Å) [10].

For the ortho [3 + 2] cycloaddition processes the lengths of the C3—C5 and C6—O7 forming bonds at the TSs are 2.147 and 2.337 Å at **TS5** and 2.063 and 2.362 Å at **TS7**, respectively, while for the meta ones the lengths of the C3—C6 and C5—O7 forming bonds at the TSs are 2.126 and 2.178 Å at **TS6** and 2.273 and 1.985 Å at **TS8**, respectively.

As for the [4 + 2] cycloadditions, the asynchronicity of the processes depends on both regioisomeric approaches and the nature of the dipolarophile. The ortho approaches are more asynchronous than the meta ones; now, the reaction with MVK leads to the most asynchronous TS, **TS7**.

At **TS5** and **TS6**, the methyl ether group adopts a similar arrangement to that at **TS1** and **TS2**, respectively. The antiperiplanar arrangement of the methyl ether group at **TS5** shows the participation of the O7 oxygen atom along the [3 + 2] cycloaddition process.

The imaginary frequency values for the TSs corresponding to the [4 + 2] cycloadditions are 384*i* (**TS1**), 564*i* (**TS2**), 456*i* (**TS3**) and 555*i* (**TS4**) $cm^{-1}$, while for the [3 + 2] ones they are 417*i* (**TS5**), 454*i* (**TS6**), 399*i* (**TS7**) and 424*i* (**TS8**) $cm^{-1}$. These low values indicate that these processes are associated with the motion of heavy atoms. For the two sorts of cycloaddition processes, the most favorable reaction channel has the TS with the lower imaginary frequency value. These results are similar to those found for related cycloaddition reactions where the more asynchronous TSs have the lower imaginary frequency [26, 37].

### *3.3 Bond order and charge analysis*

The extent of bond formation or bond breaking along a reaction pathway is provided by the concept of bond order (BO). This theoretical tool has been used to study the molecular mechanism of chemical reactions [38–41]. Values of the BO can be used to evaluate the asynchronicity of the bond formation processes and it allows us to understand the nature of the cycloaddition processes [24]. Thus, the Wiberg bond indices [42] were computed by using the NBO analysis as implemented in Gaussian 98. The results are included in Table 2.

For the [4 + 2] cycloadditions between nitroethene and MVE the BO values of the C—C and C—O forming bonds are 0.51 (C4—C5) and 0.12 (O1—C6) for the ortho **TS1** and 0.47 (C4—C6) and 0.31 (O1—C5) for the meta **TS2**. These values indicate that the ortho process is more asynchronous than the meta one. For the former, while the C4—C5 bond formation process is very advanced, the O1—C6 ones is very early. The BO value of the C6—O8 single bond at **TS1**, 1.15, shows the $\pi$ delocalization of the lone pair of the O8 oxygen atom on the C5—C6 double bond. The participation of the O8 oxygen atom along the cycloaddition process increases the nucleophilic character of MVE along the more favorable ortho approach [10, 26].

For the [4 + 2] cycloadditions between nitroethene and MVK, the BO values for the C—C and C—O forming bonds are 0.56 (C4—C5) and 0.24 (O1—C6) for the ortho **TS3** and 0.37 (C4—C6) and 0.41 (O1—C5) for the meta **TS4**. These values indicate a change in the asynchronicity of the bond formation process, which is controlled by the asymmetric MVK.

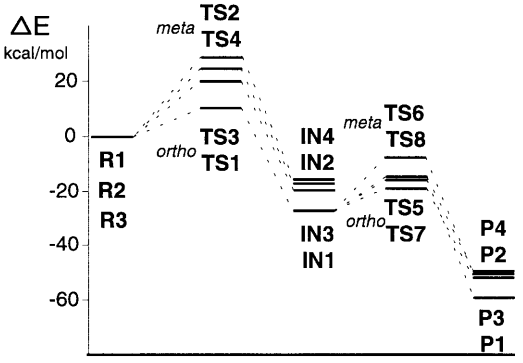


**Fig. 3.** Schematic representation of the different energy profiles for the domino cycloaddition reaction of nitroethene **R1** with methyl vinyl ether **R2** and methyl vinyl ketone **R3**

**Table 2.** Wiber bond orders (*BO*) and charge transfer (*CT*) (au) at the transition structures corresponding to the domino cycloaddition reaction between **R1** and **R2** and **R3**

| | BO | | CT |
|---|---|---|---|
| **TS1** | C4—C5 | O1—C6 | 0.34 |
| | 0.51 | 0.12 | |
| **TS2** | C4—C6 | O1—C5 | 0.19 |
| | 0.47 | 0.31 | |
| **TS3** | C4—C5 | O1—C6 | 0.16 |
| | 0.56 | 0.24 | |
| **TS4** | C4—C6 | O1—C5 | 0.11 |
| | 0.37 | 0.41 | |
| **TS5** | C3—C5 | C6—O7 | 0.09 |
| | 0.38 | 0.23 | |
| **TS6** | C3—C6 | C5—O7 | 0.00 |
| | 0.39 | 0.31 | |
| **TS7** | C3—C5 | C6—O7 | −0.07 |
| | 0.43 | 0.22 | |
| **TS8** | C3—C6 | C5—O7 | −0.06 |
| | 0.32 | 0.40 | |

For the [3 + 2] cycloadditions between the nitronate **IN1** and MVE the BO values of the C—C and C—O forming bonds are 0.38 (C3—C5) and 0.23 (C6—O7) for the ortho **TS5** and 0.39 (C3—C6) and 0.31 (C5—O7) for the meta **TS6**. For the [3 + 2] cycloadditions between **IN1** and MVK the BO values of the C—C and C—O forming bonds are 0.43 (C3—C5) and 0.22 (C6—O7) for the ortho **TS7** and 0.32 (C3—C6) and 0.40 (C5—O7) for the meta **TS8**. As for the [4 + 2] cycloadditions, the ortho TSs are more asynchronous than the meta ones. Moreover, for the reaction with **R3** there is a change in asynchronicity that is controlled by the asymmetric MVK. Finally, these data indicate that the [3 + 2] cycloadditions are less asynchronous and are earlier processes than the [4 + 2] ones [37].

Since some reactive channels present very asynchronous TSs, diradical structures could, in principle, be involved. This has been ruled out by obtaining the wave

functions of all TSs with unrestricted DFT theory. Unrestricted B3LYP/6-31G* calculations, using the keyword STABLE in Gaussian 98, predict the same TSs as the restricted B3LYP/6-31G* ones, indicating that the restricted DFT solutions are stable and allowing us to rule out the presence of more stable diradical species [26].

The natural population analysis for these TSs allows us to understand the electronic nature of these cycloaddition processes. The atomic charges at the TSs of the [4 + 2] cycloadditions were shared between the electron-rich alkene **R2** or the electron-poor alkene **R3** and the acceptor nitroalkene **R1**, while for the TSs of the [3 + 2] ones were shared between the nitronate intermediate **IN1** and **R2** or **R3**. The results are included in Table 2.

The charge transfer from the substituted alkenes to nitroethene at the TSs of the [4 + 2] cycloadditions are 0.34*e* (**TS1**), 0.19*e* (**TS2**), 016*e* (**TS3**) and 0.11*e* (**TS4**), while the charge transfer from these alkenes to the nitronate at the TSs of the [3 + 2] cycloadditions are 0.09*e* (**TS5**), 0.00*e* (**TS6**), −0.07*e* (**TS7**) and −0.06*e* (**TS8**).

For the [4 + 2] cycloadditions there is a net charge transfer from both substituted alkenes to the nitroalkene, which decreases for the cycloaddition with the electron-poor MVK. The large charge transfer found at the ortho **TS1** indicates that it has a large zwitterionic character [26]. Moreover, the larger charge transfer at **TS1** relative to that at **TS2** justifies the participation of the O8 oxygen atom along the ortho approach.

For the [3 + 2] cycloadditions there is a lower charge transfer at the TSs. While for the electron-rich MVE the charge transfer is from the alkene to the nitronate, for the electron–poor MVK it is from the nitronate to the alkene.

Thus, both BO and charge analysis indicate that the [4 + 2] cycloaddition process between nitroethene and MVE can be undertaken as a nucleophilic attack of the $\beta$ carbon of the enol ether to the conjugated position of the nitroalkene, with concomitant ring closure and without the participation of a zwitterionic intermediate to give the corresponding nitronate [26]. The lower charge transferred along the [3 + 2] cycloaddition between **IN1** and MVK together with the lower asynchronicity of the process indicate that this 1,3-dipolar cycloaddition is associated with a pericyclic process.

### *3.4 Frontier molecular orbital analysis*

Finally, the frontier molecular orbital (FMO) analysis for this domino reaction is capable of explaining the relative reactivity for these cycloadditions [26, 37]. The highest occupied molecular orbital (HOMO) and lowest unoccupied molecular orbital (LUMO) energies of **R1**, **R2**, **R3** and **IN1** are depicted in Fig. 4.

For nitroethene, **R1**, the HOMO and LUMO energies are quite low and as a consequence, the [4 + 2] cycloadditions can be considered as inverse electron demand processes [26]. Thus, the main HOMO–LUMO interactions for these cycloadditions occur between the $HOMO_{dienophile}$, **R2** or **R3**, and the $LUMO_{heterodiene}$, **R1**. If these are the dominant interactions, then the relative energies should decrease on going from **R3** to **R2**, since the $HOMO_{dienophile}$ energy increases in this series, decreasing the gap energy. For an inverse electron demand Diels–Alder cycloaddition, the presence of an electron-releasing group in the dienophile leads to a contraction of the more relevant $HOMO_{dienophile}$–$LUMO_{heterodiene}$ energy separation, increasing the reactivity [26].

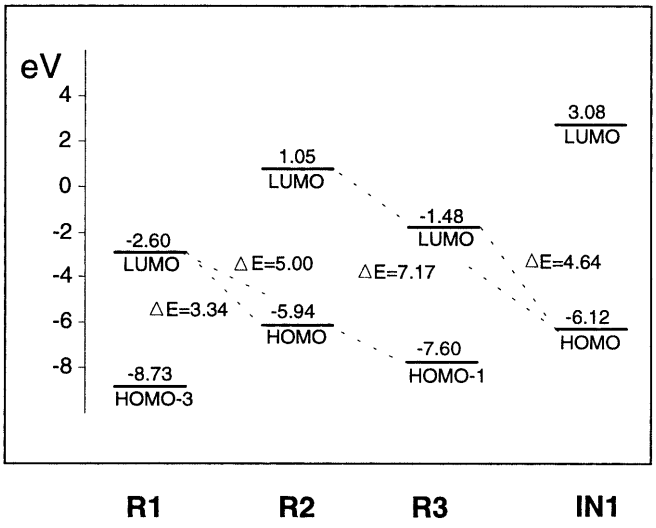


**Fig. 4.** Frontier molecular orbital interactions for the domino cycloaddition reaction between nitroethene **R1** and the enol ether **R2** and the vinyl ketone **R3**

For the nitronate **IN1** the HOMO and LUMO energies are higher than those for nitroethene. Thus, the main HOMO–LUMO interactions for the [3 + 2] cycloadditions occur between $HOMO_{dipole}$, **IN1**, and $LUMO_{dipolarophile}$, **R2** or **R3**. If these are the dominant interactions for these cycloadditions then the relative energies should decrease on going from **R2** to **R3**, since the $LUMO_{dipolarophile}$ energy decreases in this series, decreasing the gap energy. For a normal 1,3-dipolar cycloaddition, the presence of electron-withdrawing substituents in the dipolarophile leads to a contraction of the more relevant $HOMO_{dipole}$–$LUMO_{dipolarophile}$ energy separation, increasing the reactivity [37]. These facts allow us to explain the reactivity observed for this domino [4 + 2]/[3 + 2] cycloaddition.

The regioselectivity can be also rationalized in terms of FMO interactions along the ortho and meta channels. The essential difference between the reaction pathways concerns the relative orientation of the two fragments. For the [4 + 2] cycloadditions, along the ortho reaction mode, there is an arrangement in which an optimized overlap occurs between the HOMO of the dienophile fragment (associated with the $\pi$ system of the substituted ethene) and the LUMO of the heterodiene fragment (associated with $\pi^*$ system of nitroethene). This is due to the biggest molecular orbital coefficients at the C4 and C5 atoms in these FMOs [26]. However, different behavior is found for the [3 + 2] cycloadditions since the B3LYP/6-31G* calculation gives a slightly bigger molecular orbital coefficient at the O7 oxygen atom than at the C3 carbon atom of the nitronate group, justifying a low meta regioselectivity. This disagreement can be

avoided by considering that along the most favorable ortho channel a polarization of the nitronate HOMO can take place when both reactants, dipole and dipolarophile, are close [44]. This polarization can increase the molecular orbital coefficient at the C3 atom relative to that at the O7 one, favoring the overlap between dipole and dipolarophile along the ortho approach.

## 4 Conclusions

The molecular mechanism for the domino intermolecular [4 + 2]/[3 + 2] cycloaddition reactions of nitroalkenes with vinyl ethers and vinyl ketones has been characterized using DFT methods with the B3LYP functional and the 6-31G* basis set.

These domino processes comprise two consecutive cycloaddition reactions: the first one is a [4 + 2] cycloaddition of the nitroalkene with the vinyl ether to give a nitronate intermediate, whereas the second one is a [3 + 2] cycloaddition of this intermediate with the vinyl ketone to afford the final nitroso acetal adduct.

The two consecutive cycloadditions present total chemo- and regioselectivity. While the [4 + 2] cycloaddition reaction takes place along the attack of the electron-rich alkene to the nitroalkene, the [3 + 2] one takes place along the attack of the electron-poor alkene to the corresponding nitronate intermediate. Moreover, the lower chemoselectivity found for the second [3 + 2] cycloaddition accounts for these domino reactions taking place without the participation of the electron-poor alkene. Both cycloadditions are ortho regioselective. This DFT study is in complete agreement with the experimental results, allowing the observed chemo- and regioselectivity for these domino reactions to be explained.

*Acknowledgements*. This work was supported by research funds provided by the Conselleria de Cultura Educació i Ciéncia, Generalitat Valenciana (Project GV97-CB-11-86). All calculations were performed on a Cray-Silicon Graphics Origin 2000 with 64 processors of the Servicio de Informática de la Universidad de Valencia. I am most indebted to this center for providing us with computer capabilities.

## References

1. Tietze LF (1996) Chem Rev 96: 115
2. Tietze LF (1995) Chem Ind 453
3. Tietze LF, Beifuss U (1993) Angew Chem Int Ed Engl 32: 131
4. Carruthers W (1990) Cycloaddition reactions in organic synthesis. Pergamon, Oxford
5. Denmark SE, Thorarensen A (1996) Chem Rev 96: 137
6. Winkler JD (1996) Chem Rev 96: 167
7. Avalos M, Babiano R, Cintas P, Higes FJ, Jiménez JL, Palacios JC, Silva MA (1996) J Org Chem 61: 1880
8. Avalos M, Babiano R, Cintas P, Jiménez JL, Palacios JC, Silva MA (1998) Chem Commun 459
9. Avalos M, Babiano R, Cintas P, Higes FJ, Jiménez JL, Palacios JC, Silva MA (1999) J Org Chem 64: 1494
10. Domingo LR, Picher MT, Andrés J (1999) J Phys Org Chem 12: 24
11. Parr RG, Yang W (1989) Density functional theory of atoms and molecules. Oxford University Press, New York
12. Ziegler T (1991) Chem Rev 91: 651
13. Stanton RV, Merz KM (1994) J Chem Phys 100: 434
14. Carpenter JE, Sosa CP (1994) J Mol Struct (THEOCHEM) 311: 325
15. Baker J, Muir M, Andzelm J (1995) J Chem Phys 102: 2036
16. Jursic B, Zdravkovski Z (1995) J Chem Soc Perkin Trans 2: 1223
17. Goldstein E, Beno B, Houk KN (1996) J Am Chem Soc 118: 6036
18. Branchadell V (1997) Int J Quantum Chem 61: 381
19. Sbai A, Branchadell V, Ortuño RM, Oliva A (1997) J Org Chem 62: 3049
20. Branchadell V, Font J, Moglioni AG, Ochoa de Echaguen C, Oliva A, Ortuno RM, Veciana J, Vidal Gancedo J (1997) J Am Chem Soc 119: 9992
21. García JI, Martínez-Merino V, Mayoral JA, Salvatella L (1998) J Am Chem Soc 120: 2415
22. Tietze LF, Pfeiffer T, Schuffenhauer A (1998) Eur J Org Chem 2773
23. Domingo LR, Arnó M, Andrés J (1998) J Am Chem Soc 120: 1617
24. Domingo LR, Picher MT, Zaragozá RJ (1998) J Org Chem 63: 9183
25. Morao I, Lecea B, Cossió FP (1997) J Org Chem 62: 7033
26. Domingo LR, Arnó M, Andrés J (1999) J Org Chem 64: 5867
27. Becke AD (1993) J Chem Phys 98: 5648
28. Lee C, Yang W, Parr RG (1988) Phys Rev B 37: 785
29. Hehre WJ, Radom L, Schleyer PvR, Pople JA (1986) Ab initio molecular orbital Theory. Wiley, New York
30. Schlegel HB (1982) J Comput Chem 3: 214
31. Schlegel HB (1994) In: Yarkony DR (ed) Modern electronic structure theory. World Scientific, Singapore
32. Reed AE, Weinstock RB, Weinhold F (1985) J Chem Phys 83: 735
33. Reed AE, Curtiss LA, Weinhold F (1988) Chem Rev 88: 899
34. Frisch MJ, Trucks GW, Schlegel HB, Scuseria GE, Robb MA, Cheeseman JR, Zakrzewski VG, Montgomery JA Jr , Stratmann RE, Burant J, Dapprich S, Millam JM, Daniels AD, Kudin KN, Strain MC, Farkas O, Tomasi J, Barone V, Cossi M, Cammi R, Mennucci B, Pomelli C, Adamo C, Clifford S, Ochterski J, Petersson GA, Ayala PY, Cui Q, Morokuma K, Malick DK, Rabuck AD, Raghavachari K, Foresman JB, Cioslowski J, Ortiz JV, Stefanov BB, Liu, G, Liashenko A, Piskorz P, Komaromi I, Gomperts R, Martin RL, Fox DJ, Keith T, Al-Laham MA, Peng CY, Nanayakkara A, Gonzalez C, Challacombe M, Gill PMW, Johnson B, Chen W, Wong MW, Andres JL, Gonzalez C, Head-Gordon M, Replogle ES, Pople JA (1998) Gaussian 98, revision A.6. Gaussian, Pittsburgh, Pa
35. Perrin CL, Armstrong KB, Fabian MA (1994) J Am Chem Soc 116: 715
36. Gothelf KV, Jorgensen KA (1998) Chem Rev 98: 863
37. Domingo LR (1999) J Org Chem 64: 3922
38. Varandas AJC, Formosinho SJF (1986) J Chem Soc Faraday Trans 2: 282
39. Lendvay G (1988) J Mol Struct (THEOCHEM) 167: 331
40. Lendvay G (1989) J Phys Chem 93: 4422
41. Lendvay G (1994) J Phys Chem 98: 6098
42. Wiberg KB (1968) Tetrahedron 24: 1083
43. Kahn SD, Hehre WJ, Pople JA (1987) J Am Chem Soc 109: 1871
44. Contreras R, Domingo LR, Andrés J, Pérez P, Tapia O (1999) J Phys Chem A 103: 1367